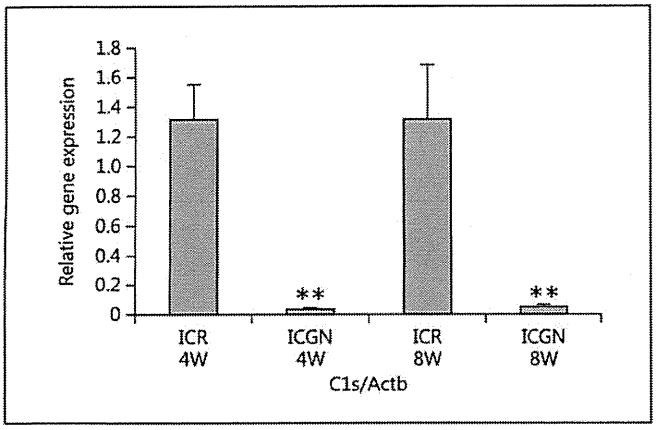

Fig. 3. Expression level of *C1s* mRNA in the livers was assessed by quantitative PCR. *C1s* mRNA level was markedly low in ICGN mice as compared with age-matched ICR mice at both 4 and 8 weeks of age. Each value is averaged among 3 mice with the error bar displaying the standard deviation. ** $p < 0.01$ compared with age-matched ICR mice.

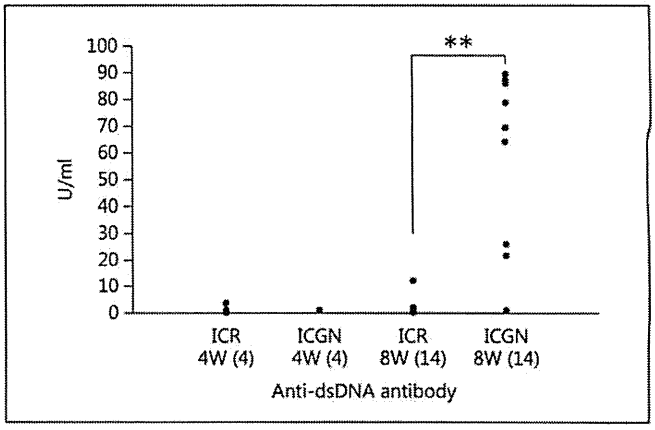

Fig. 4. Serum anti-dsDNA antibody was measured by ELISA in 4- and 8-week-old ICGN mice and age-matched ICR mice. A markedly high level of serum anti-dsDNA antibody was observed in ICGN mice as compared with ICR mice. ** $p < 0.01$ compared with age-matched ICR mice. The numbers of mice examined are given in parentheses.

Table 5. Affected genes on complement system pathway

Probe set ID	Gene symbol	Entrez gene name	Fold change	
			4 weeks	8 weeks
1417381_at	*C1qa*	Complement component 1, q subcomponent, α polypeptide	2.5*	4.8
1417063_at	*C1qb*	Complement component 1, q subcomponent, β polypeptide	2.6*	4.7
1437726_x_at	*C1qb*	Complement component 1, q subcomponent, β polypeptide	2.4	6.1
1449401_at	*C1qc*	Complement component 1, q subcomponent, C chain	2.6*	5.5
1424041_s_at	*C1s*	Complement component 1, s subcomponent	−45.1*	−26.8*
1441912_x_at	*C2*	Complement component 2 (within H-2S)	1.1	2.2*
1423954_at	*C3*	Complement component 3	4.3	20.7
1419483_at	*C3ar1*	Complement component 3a receptor 1	2.5*	2.1
1442082_at	*C3ar1*	Complement component 3a receptor 1	2.5	4.8*
1450876_at	*Cfh*	Complement component factor h	1.2	3.0*
1416625_at	*Serping1*	Serine (or cysteine) peptidase inhibitor, clade G, member 1	1.2	2.4*

* $p < 0.01$ compared with age-matched ICR mice.

Pathway Analysis

Canonical pathway analysis using IPA was conducted to identify biological pathways which were significantly altered in the kidneys of 4- and 8-week-old ICGN mice. 41 pathways were significantly altered in ICGN mice (table 4). Approximately 76% of the altered pathways (31 of 41 pathways) were categorized into 'humoral immune response', 'cellular immune response' and/or 'cytokine signaling'.

Quantitative PCR

Of the 37 overlapping transcripts in renal cortical tissue, the *C1s* gene expression appeared to be markedly altered (reduced) compared to the other transcripts (table 3). Therefore, quantitative PCR was conducted to measure *C1s* mRNA in the livers where C1s protein is primarily produced. Quantitative PCR showed that *C1s* mRNA level was also markedly low in ICGN mice liver as compared with age-matched ICR mice (fig. 3).

Table 6. Representative genes upregulated significantly in ICGN mouse kidney at 8 weeks of age

Probe set ID	Gene symbol	Entrez gene name	Fold change	
			4 weeks	8 weeks
MHC class II				
1435290_x_at	*H2-Aa*	Histocompatibility 2, class II antigen A, α	3.4	3.2*
1438858_x_at	*H2-Aa*	Histocompatibility 2, class II antigen A, α	5.1*	5.5*
1443687_x_at	*H2-DMb2*	Histocompatibility 2, class II, locus Mb2	3.3*	16.6
1422891_at	*H2-Ea-ps /// LOC100504404*	Histocompatibility 2, class II antigen E α, pseudogene /// h-2 class II histocompatibility antigen, E-K α chain-like	9.5	15.9*
1422892_s_at	*H2-Ea-ps /// LOC100504404*	Histocompatibility 2, class II antigen E α, pseudogene /// h-2 class II histocompatibility antigen, E-K α chain-like	8.9	29.9*
1417025_at	*H2-Eb1*	Histocompatibility 2, class II antigen E β	3.6	3.4*
1425519_a_at	*Cd74*	CD74 antigen (invariant polypeptide of major histocompatibility complex, class II antigen-associated)	3.3	5.2*
CD markers reported to be preferentially expressed in hematopoietic lineages				
1417268_at	*Cd14*	CD14 antigen	2.0	3.7*
1437502_x_at	*Cd24a*	CD24a antigen	−1.2	2.1*
1449473_s_at	*Cd40*	CD40 antigen	1.3	2.9*
1449164_at	*Cd68*	CD68 antigen	1.8	3.3*
1426112_a_at	*Cd72*	CD72 antigen	2.0*	2.3
1425519_a_at	*Cd74*	CD74 antigen (invariant polypeptide of major histocompatibility complex, class II antigen-associated)	3.3	5.2*
1420404_at	*Cd86*	CD86 antigen	3.0	2.9*
1449858_at	*Cd86*	CD86 antigen	2.8*	3.1
Collagen				
1455494_at	*Col1a1*	Collagen, type I, α 1	−1.4	2.7*
1423110_at	*Col1a2*	Collagen, type I, α 2	−1.3	4.0*
1450857_a_at	*Col1a2*	Collagen, type I, α 2	−1.3	2.5*
1427883_a_at	*Col3a1*	Collagen, type III, α 1	−1.4	2.5*
1427884_at	*Col3a1*	Collagen, type III, α 1	−1.5	4.1*
1416740_at	*Col5a1*	Collagen, type V, α 1	−1.1	2.4*
1416741_at	*Col5a1*	Collagen, type V, α 1	1.2	3.2*
1422437_at	*Col5a2*	Collagen, type V, α 2	−1.0	3.5*
1418441_at	*Col8a1*	Collagen, type VIII, α 1	1.7	2.9*
1455627_at	*Col8a1*	Collagen, type VIII, α 1	1.2	3.6*
1427391_a_at	*Col12a1*	Collagen, type XII, α 1	1.3	3.0*
1434411_at	*Col12a1*	Collagen, type XII, α 1	1.6	3.8*
1418237_s_at	*Col18a1*	Collagen, type XVIII, α 1	1.6	4.0*
1426955_at	*Col18a1*	Collagen, type XVIII, α 1	1.5	3.0*

* $p < 0.01$ compared with age-matched ICR mice.

ELISA of Anti-dsDNA Antibody

Serum anti-dsDNA antibody was measured in 4- and 8-week-old ICGN mice and age-matched ICR mice. ELISA detected a markedly high level of serum anti-dsDNA antibody in 8-week-old ICGN mice as compared with age-matched ICR mice (ICR vs. ICGN: 1.0 ± 3.0 vs. 50.0 ± 38.8 U/ml) (fig. 4).

Discussion

To identify additional associative factors for nephrotic syndrome in ICGN mice, and to better understand onset mechanism of nephrotic syndrome in ICGN mice, microarray analysis was conducted with the renal cortex from 4- and 8-week-old ICGN and ICR mice. As compared with age-matched ICR mice kidney, 252 and 807

transcripts met the filtering criteria in the kidneys of 4- and 8-week-old ICGN mice. The number of differentially expressed transcripts increased with progression of nephrotic syndrome. Canonical pathway analysis identified 41 significantly affected biological pathways in the kidneys of 4- and/or 8-week-old ICGN mice (table 4). The fact that approximately 76% of the affected pathways (31 of 41 pathways) were categorized into 'humoral immune response', 'cellular immune response' and/or 'cytokine signaling' raises the possibility that immune-related pathways may play a key role in nephrotic syndrome in ICGN mice. The 37 differentially expressed transcripts (table 3) are considered to be candidates for associative factors for nephrotic syndrome in ICGN mice. The most drastically altered gene was *C1s*, which is involved in complement system. In humans, C1s deficiency has been reported to associate with lupus nephritis [13–17]. Although it has not been fully understood what activity of the early proteins in the classical pathway of complement protects normal humans from development of lupus nephritis, clearance of immune complexes is thought to be a candidate activity [18]. The C1 complex of complement is composed of C1q, C1r, and C1s subcomponents, and is essential to initiate the classical pathway of complement activation. The classical pathway plays a key role in the clearance of circulating immune complexes [19, 20]. In deficiency of the classical pathway, circulating immune complexes might escape normal elimination from plasma and deposit in tissues instead. Then the immune complexes might cause inflammation and release of autoantigens, which in turn could stimulate an autoimmune response. Quantitative PCR revealed that *C1s* gene expression level in ICGN mice liver, where C1s is mainly produced, was markedly reduced as compared to ICR mice (fig. 3). Pathway analysis also detected 'complement system' pathway as significantly altered pathway in the kidneys of ICGN mice at both 4 and 8 weeks of age (table 4). Some of the genes on the 'complement system' pathway were altered in ICGN mice renal cortical tissue; however, the *C1s* gene was the most drastically altered (table 5). Decreased expression level of *C1s* gene was already present at 4 weeks of age, when only slight or mild histopathological changes were observed, and persisted to 8 weeks of age. Deposition of immune complexes in glomeruli is a common finding in the inflammatory glomerulonephritis, including lupus nephritis. Anti-dsDNA antibody is diagnostic for systemic lupus erythematosus and its specificity is 97.4% [21]. Deposition of IgA, IgG and IgM in glomeruli, and marked high level of serum anti-dsDNA antibody observed in ICGN mice indicate that the low expression level of *C1s* gene associates with nephrotic syndrome in ICGN mice.

It has been suggested that deletion mutation of *Tns2* is responsible for nephrotic syndrome in ICGN mice and *Tns2* is expressed in podocytes and tubular epithelial cells in normal mice but not in ICGN mice [8]. We also detected decreased expression level of *Tns2* gene in ICGN mice kidney. OSMR is one of the receptor proteins for Oncostatin M (OSM) which has both pro-inflammatory properties [22] and anti-inflammatory properties [23]. In the kidneys, gene expression of *Osmr* was detected in endothelial cells of peritubular capillaries [24]. OSM has been demonstrated to regulate expressions of tissue inhibitors of metalloproteinases (TIMPs) and matrix metalloproteinases (MMPs) in various types of cells [25–27]. We previously reported the excessive accumulation of extracellular matrix components (type I, III and IV collagen, fibronectin, laminin and tenascin) and decreased expressions and/or activities of matrix metalloproteinase (MMP)-1, MMP-2, MMP-9 and MMP-12 [28–32]. The upregulation of *Osmr* gene may relate to the decreased expressions and/or activities of MMPs in ICGN mice kidneys. Chemokine (C-C motif) receptor 5 *(Ccr5)* gene encodes a member of β-chemokine receptor family, and is preferentially expressed in T cells and macrophages. In humans, CCR5-positive mononuclear cells were identified in areas of interstitial infiltration in biopsies of chronic glomerulonephritis, interstitial nephritis, and transplant rejection [33]. In murine lupus nephritis (MRL/lpr mice), microarray analysis revealed increased expression levels in many genes including *Ccr5* preferentially or exclusively expressed in hematopoietic lineages [34]. Therefore, an increased expression level of *Ccr5* gene in ICGN mice kidney was considered to be related to leukocyte accumulation. Histocompatibility 2, D region locus 1 *(H2-D1)* is a member of major histocompatibility complex (MHC) class I which plays a central role in the immune system by presenting endogenous antigen. MHC class I is expressed in all nucleated cell and induced by inflammatory cytokines including interferon (IFN)-γ and tumor necrosis factor (TNF)-α [35, 36]. Therefore, the highly expressed MHC class I gene in ICGN mice kidney was possibly derived from cytokine-stimulated renal resident cells. Similarly, some of the 37 genes (histocompatibility 2, class II antigen A, α *(H2-Aa)* [37], class II transactivator *(Ciita)* [38], ceruloplasmin *(Cp)* [39], cathepsin S *(Ctss)* [40], guanylate-binding protein 2 *(Gbp2)* [41], myelocytomatosis oncogene *(Myc)* [42], TNF-α-induced protein 3 *(Tnfaip3)* [43], and pleckstrin *(Plek)* [44]) were reported to be induced by IFN-γ,

TNF-α and/or interleukin-6. To understand the association between the remaining differentially expressed 37 transcripts and nephrotic syndrome in ICGN mice, further investigations are needed.

In several types of CD (cluster of differentiation) markers and MHC class II, preferentially or exclusively expressed in immune cells, the expression levels were increased in ICGN mice kidney, especially at 8 weeks of age when immune cell infiltration was aggravated (table 6). A part of increased gene expressions in 8-week-old ICGN mice kidney was considered to reflect aggravation of inflammatory cell infiltration. Gene expression levels of some collagen subtypes were also increased especially at 8 weeks of age (table 6) and it is considered to be related to fibrosis associated with progression of nephrotic syndrome.

In summary, our results suggest that the immune system, especially the complement system, is associated with nephrotic syndrome in ICGN mice. We identified a low expression level of *C1s* gene as an additional associative factor for nephrotic syndrome in ICGN mice. Further studies are needed to elucidate the mechanism of the marked decrease in *C1s* gene expression and the role of the complement system in the onset of nephrotic syndrome in ICGN mice.

Acknowledgments

The authors would like to thank Dr. Marlowe Schneidkraut and Dr. Kumiko Nishihara for their scientific advice. We are also grateful to Mr. Kenji Nakano, Ms. Mayumi Murata and Ms. Tsugiko Yamasaki for specimen preparation for histopathology and immunohistochemistry.

References

1 Ogura A, Asano T, Matsuda J, Noguchi Y, Yamamoto Y, Takano K, Nakagawa M: Development of nephrotic ICGN mice – the origin, reproductive ability, and incidence of glomerulonephritis. Jikken Dobutsu 1989;38:349–352.

2 Ogura A, Asano T, Matsuda J, Takano K, Nakagawa M, Fukui M: Characteristics of mutant mice (ICGN) with spontaneous renal lesions: a new model for human nephrotic syndrome. Lab Anim 1989;23:169–174.

3 Ogura A, Asano T, Suzuki O, Yamamoto Y, Noguchi Y, Kawaguchi H, Yamaguchi Y: Hereditary nephrotic syndrome with progression to renal failure in a mouse model (ICGN strain): clinical study. Nephron 1994;68:239–244.

4 Ogura A, Asano T, Matsuda J, Fujimura H: Evolution of glomerular lesions in nephrotic ICGN mice: serial biopsy study with electron microscopy. J Vet Med Sci 1991;53:513–515.

5 Ogura A, Asano T, Matsuda J, Koura M, Nakagawa M, Kawaguchi H, Yamaguchi Y: An electron microscopic study of glomerular lesions in hereditary nephrotic mice (ICGN strain). Virchows Arch A Pathol Anat Histopathol 1990;417:223–228.

6 Ogura A, Fujimura H, Asano T, Koura M, Naito I, Kobayashi Y: Early ultrastructural glomerular alterations in neonatal nephrotic mice (ICGN strain). Vet Pathol 1995;32:321–323.

7 Okamoto M, Yokoi N, Seriklawa T, Tajima M, Kurosawa T: Linkage mapping of the mouse nephrosis (nep) gene to chromosome 15. J Vet Med Sci 2001;63:1347–1350.

8 Cho AR, Uchio-Yamada K, Torigai T, Miyamoto T, Miyoshi I, Matsuda J, Kurosawa T, Kon Y, Asano A, Sasaki N, Agui T: Deficiency of the tensin2 gene in the ICGN mouse: an animal model for congenital nephrotic syndrome. Mamm Genome 2006;17:407–416.

9 Weigt C, Gaertner A, Wegner A, Korte H, Meyer HE: Occurrence of an actin-inserting domain in tensin. J Mol Biol 1992;227:593–595.

10 Nishino T, Sasaki N, Nagasaki K, Ahmad Z, Agui T: Genetic background strongly influences the severity of glomerulosclerosis in mice. J Vet Med Sci 2010;72:1313–1318.

11 Nishino T, Sasaki N, Nagasaki K, Ichii O, Kon Y, Agui T: The 129 genetic background affects susceptibility to glomerulosclerosis in tensin2-deficient mice. Biomed Res 2012;33:53–56.

12 Tamura K, Ono A, Miyagishima T, Nagao T, Urushidani T: Comparison of gene expression profiles among papilla, medulla and cortex in rat kidney. J Toxicol Sci 2006;31:449–469.

13 Amano MT, Ferriani VP, Florido MP, Reis ES, Delcolli MI, Azzolini AE, Assis-Pandochi AI, Sjoholm AG, Farah CS, Jensenius JC, Isaac L: Genetic analysis of complement c1s deficiency associated with systemic lupus erythematosus highlights alternative splicing of normal c1s gene. Mol Immunol 2008;45:1693–1702.

14 Bienaime F, Quartier P, Dragon-Durey MA, Fremeaux-Bacchi V, Bader-Meunier B, Patey N, Salomon R, Noel LH: Lupus nephritis associated with complete c1s deficiency efficiently treated with rituximab: a case report. Arthritis Care Res (Hoboken) 2010;62:1346–1350.

15 Dragon-Durey MA, Quartier P, Fremeaux-Bacchi V, Blouin J, de Barace C, Prieur AM, Weiss L, Fridman WH: Molecular basis of a selective c1s deficiency associated with early onset multiple autoimmune diseases. J Immunol 2001;166:7612–7616.

16 Inoue N, Saito T, Masuda R, Suzuki Y, Ohtomi M, Sakiyama H: Selective complement c1s deficiency caused by homozygous four-base deletion in the c1s gene. Hum Genet 1998;103:415–418.

17 Suzuki Y, Ogura Y, Otsubo O, Akagi K, Fujita T: Selective deficiency of c1s associated with a systemic lupus erythematosus-like syndrome. Report of a case. Arthritis Rheum 1992;35:576–579.

18 Walport MJ, Davies KA: Complement and immune complexes. Res Immunol 1996;147:103–109.

19 Walport MJ: Complement. First of two parts. N Engl J Med 2001;344:1058–1066.

20 Walport MJ: Complement. Second of two parts. N Engl J Med 2001;344:1140–1144.

21 Kavanaugh AF, Solomon DH: Guidelines for immunologic laboratory testing in the rheumatic diseases: anti-DNA antibody tests. Arthritis Rheum 2002;47:546–555.

22 Modur V, Feldhaus MJ, Weyrich AS, Jicha DL, Prescott SM, Zimmerman GA, McIntyre TM: Oncostatin M is a proinflammatory mediator. In vivo effects correlate with endothelial cell expression of inflammatory cytokines and adhesion molecules. J Clin Invest 1997;100:158–168.

23 Wallace PM, MacMaster JF, Rouleau KA, Brown TJ, Loy JK, Donaldson KL, Wahl AF: Regulation of inflammatory responses by oncostatin M. J Immunol 1999;162:5547–5555.

24 Tamura S, Morikawa Y, Tanaka M, Miyajima A, Senba E: Developmental expression pattern of oncostatin M receptor β in mice. Mech Dev 2002;115:127–131.
25 Gatsios P, Haubeck HD, Van de Leur E, Frisch W, Apte SS, Greiling H, Heinrich PC, Graeve L: Oncostatin M differentially regulates tissue inhibitors of metalloproteinases TIMP-1 and TIMP-3 gene expression in human synovial lining cells. Eur J Biochem 1996; 241:56–63.
26 Korzus E, Nagase H, Rydell R, Travis J: The mitogen-activated protein kinase and JAK-STAT signaling pathways are required for an oncostatin M-responsive element-mediated activation of matrix metalloproteinase-1 gene expression. J Biol Chem 1997;272:1188–1196.
27 Li WQ, Zafarullah M: Oncostatin M up-regulates tissue inhibitor of metalloproteinases-3 gene expression in articular chondrocytes via de novo transcription, protein synthesis, and tyrosine kinase- and mitogen-activated protein kinase-dependent mechanisms. J Immunol 1998;161:5000–5007.
28 Uchio K, Manabe N, Kinoshita A, Tamura K, Miyamoto M, Ogura A, Yamamoto Y, Miyamoto H: Abnormalities of extracellular matrices and transforming growth factor-β_1 localization in the kidney of the hereditary nephrotic mice (ICGN strain). J Vet Med Sci 1999;61:769–776.
29 Uchio K, Manabe N, Tamura K, Miyamoto M, Yamaguchi M, Ogura A, Yamamoto Y, Miyamoto H: Decreased matrix metalloproteinase activity in the kidneys of hereditary nephrotic mice (ICGN strain). Nephron 2000;86:145–151.
30 Uchio K, Sawada K, Manabe N: Expression of macrophage metalloelastase (MMP-12) in podocytes of hereditary nephrotic mice (ICGN strain). J Vet Med Sci 2009;71:305–312.
31 Uchio-Yamada K, Manabe N, Goto Y, Anann S, Yamamoto Y, Takano K, Ogura A, Matsuda J: Decreased expression of matrix metalloproteinases and tissue inhibitors of metalloproteinase in the kidneys of hereditary nephrotic (ICGN) mice. J Vet Med Sci 2005;67:35–41.
32 Uchio-Yamada K, Manabe N, Yamaguchi M, Akashi N, Goto Y, Yamamoto Y, Ogura A, Miyamoto H: Localization of extracellular matrix receptors in ICGN mice, a strain of mice with hereditary nephrotic syndrome. J Vet Med Sci 2001;63:1171–1178.
33 Segerer S, Mac KM, Regele H, Kerjaschki D, Schlondorff D: Expression of the C-C chemokine receptor 5 in human kidney diseases. Kidney Int 1999;56:52–64.
34 Teramoto K, Negoro N, Kitamoto K, Iwai T, Iwao H, Okamura M, Miura K: Microarray analysis of glomerular gene expression in murine lupus nephritis. J Pharmacol Sci 2008; 106:56–67.
35 Hawkins NJ, Ward RL, Wakefield D: Cytokine-mediated induction of HLA antigen expression on human glomerular mesangial cells. Cell Immunol 1994;155:493–500.
36 Ikeda M, Minota S, Kano S: Regulation of MHC class I expression by inflammatory cytokines in rat mesangial cells. Nephron 1997; 76:90–95.
37 Rohn WM, Lee YJ, Benveniste EN: Regulation of class II MHC expression. Crit Rev Immunol 1996;16:311–330.
38 Londhe P, Davie JK: Gamma interferon modulates myogenesis through the major histocompatibility complex class II transactivator, CIITA. Mol Cell Biol 2011;31:2854–2866.
39 Mazumder B, Mukhopadhyay CK, Prok A, Cathcart MK, Fox PL: Induction of ceruloplasmin synthesis by IFN-γ in human monocytic cells. J Immunol 1997;159:1938–1944.
40 Beers C, Honey K, Fink S, Forbush K, Rudensky A: Differential regulation of cathepsin S and cathepsin L in interferon-γ-treated macrophages. J Exp Med 2003;197:169–179.
41 Degrandi D, Konermann C, Beuter-Gunia C, Kresse A, Wurthner J, Kurig S, Beer S, Pfeffer K: Extensive characterization of IFN-induced GTPases mGBP1 to mGBP10 involved in host defense. J Immunol 2007;179:7729–7740.
42 Rubio N, Torres C: Interferon-γ induces proliferation but not apoptosis in murine astrocytes through the differential expression of the myc proto-oncogene family. Brain Res Mol Brain Res 1999;71:104–110.
43 Lee EG, Boone DL, Chai S, Libby SL, Chien M, Lodolce JP, Ma A: Failure to regulate TNF-induced NF-κB and cell death responses in A20-deficient mice. Science 2000;289:2350–2354.
44 Brumell JH, Howard JC, Craig K, Grinstein S, Schreiber AD, Tyers M: Expression of the protein kinase C substrate pleckstrin in macrophages: association with phagosomal membranes. J Immunol 1999;163:3388–3395.

Exp. Anim. 62(3), 267–273, 2013

—Original—

Zygosity Determination in Hairless Mice by PCR Based on *Hr*^{hr} Gene Analysis

Osamu SUZUKI, Minako KOURA, Yoko NOGUCHI, Kozue UCHIO-YAMADA, and Junichiro MATSUDA

Laboratory of Animal Models for Human Diseases, National Institute of Biomedical Innovation, 7–6–8 Saito-Asagi, Ibaraki, Osaka 567-0085, Japan

Abstract: We analyzed the *Hr* gene of a hairless mouse strain of unknown origin (HR strain, http://animal.nibio.go.jp/e_hr.html) to determine whether the strain shares a mutation with other hairless strains, such as HRS/J and Skh:HR-1, both of which have an *Hr*^{hr} allele. Using PCR with multiple pairs of primers designed to amplify multiple overlapping regions covering the entire *Hr* gene, we found an insertion mutation in intron 6 of mutant *Hr* genes in HR mice. The DNA sequence flanking the mutation indicated that the mutation in HR mice was the same as that of *Hr*^{hr} in the HRS/J strain. Based on the sequence, we developed a genotyping method using PCR to determine zygosities. Three primers were designed: S776 (GGTCTCGCTGGTCCTTGA), S607 (TCTGGAACCAGAGTGACAGACAGCTA), and R850 (TGGGCCACCATGGCCAGATTTAACACA). The S776 and R850 primers detected the *Hr*^{hr} allele (275-bp amplicon), and S607 and R850 identified the wild-type *Hr* allele (244-bp amplicon). Applying PCR using these three primers, we confirmed that it is possible to differentiate among homozygous *Hr*^{hr} (longer amplicons only), homozygous wild-type *Hr*(shorter amplicons only), and heterozygous (both amplicons) in HR and Hos:HR-1 mice. Our genomic analysis indicated that the HR, HRS/J, and Hos:HR-1 strains, and possibly Skh:HR-1 (an ancestor of Hos:HR-1) strain share the same *Hr*^{hr} gene mutation. Our genotyping method will facilitate further research using hairless mice, and especially immature mice, because pups can be genotyped before their phenotype (hair coat loss) appears at about 2 weeks of age.

Key words: hairless, genome, genotyping, mice, zygosity

Introduction

Many hairless mouse strains such as HRS/J and Skh:HR-1 are often used in studies of skin, cancer, and immunology by Benavides *et al.* [3] and Sundberg [12]. At our institute, we have been maintaining a hairless mouse strain of unknown origin called HR (http://animal.nibio.go.jp/e_hr.html). It was introduced from a University in California (there is no precise university name in our records) to Yokohama City University in 1964. The strain was then introduced in 1965 to the Institute of Medical Science of the University of Tokyo, where a mutated *Hairless* gene from this strain was transferred into a BALB/c background. The strain was introduced to our institute (National Institutes of Health, at the time of introduction) in 1981. The HRS/J strain was established in 1964 by inbreeding mice obtained by crossing offspring of the hairless mice first found in London [4] with BALB/c mice at the Jackson Laboratory (http://jaxmice.jax.org/strain/000673.html). In addition, the Hos:HR-1 strain was established in 1987 at Hoshino Laboratory Animals Inc. by inbreeding the Skh:HR-1

(Received 18 February 2013 / Accepted 30 March 2013)

Address corresponding: O. Suzuki, Laboratory of Animal Models for Human Diseases, National Institute of Biomedical Innovation, 7–6–8 Saito-Asagi, Ibaraki, Osaka 567-0085, Japan

outbred strain, which had been established at Temple University by crossing the CBA strain (http://www.hoshino-lab-animals.co.jp/english/products/HR1-en.html) with hairless mice of unknown origin from Sandra Biological Supply. It remains unknown whether HR mice carry the same mutation as other hairless strains, such as HRS/J and Skh:HR-1 (Hos:HR-1), even though the three strains show the same phenotype.

The hairless mutation was first found in a mouse in 1924 [4]. This mutation is an autosomal recessive mutation (Hr^{hr}) in the *Hr* gene [11]. Murine *Hr* localizes to the 70-Mb position of mouse chromosome 14, and contains 19 exons [5]. The *hr* mutation is caused by an insertion of the murine leukemia virus into intron 6 [11]. Both HRS/J and Skh:HR-1 (Hos:HR-1) carry this mutation [10]. Homozygous mutants (Hr^{hr}/Hr^{hr}) show normal development of the first hair coat (first hair cycle). Starting at 2 weeks of age, they lose their hair coat rapidly and completely due to an abnormal second hair cycle [4, 13]. At weaning (~3 weeks of age), they are completely hairless. In general, females homozygous for Hr^{hr} often fail to nurse their litters due to abnormal lactation (except Hos:HR-1 homozygous females, which show normal lactation; thus, this low nursing activity is thought to depend on the genetic background, not the *Hr* mutation itself). Therefore, most hairless strains have been maintained by mating heterozygous females (normal hair coat) and homozygous males (no hair coat). In this case, pups are a mixture of heterozygous and homozygous mutants. Homozygous mutants cannot be distinguished from heterozygous ones based on appearance alone because they both have coats before 2 weeks of age. Hence, a genotyping method is also needed if younger mice are to be used.

We analyzed the *Hr* gene of the HR strain maintained at our institute to determine if its *Hr* mutation (tentatively called "Hr^{x}") is the same as that (Hr^{hr}) of other hairless strains (such as HRS/J). In addition, we developed a PCR method to determine the genotypes of pups before the phenotype (hair coat loss) appears (~2 weeks of age) based on the sequence information of HR mice.

Materials and Methods

Hairless mice

At our institute, HR mice (nbio#: nbio003) have been maintained by crossing heterozygous females (Hr/Hr^{x}) and homozygous males (Hr^{x}/Hr^{x}). Wild-type HR mice (*Hr/Hr*), which had no mutated HR (Hr^{x}) alleles, were produced by crossing heterozygous females and males. Hos:HR-1 mice homozygous for hairless genes were purchased from Hoshino Laboratory Animals, Inc. (Bando, Japan) through Japan SLC, Inc. (Hamamatsu, Japan) and used for genotyping tests. All mice were housed under specific pathogen-free conditions with food (CMF, Oriental Yeast Co., Ltd., Tokyo, Japan) and water provided *ad libitum*. All animal experiments were conducted in accordance with the guidelines for animal experiments of the National Institute of Infectious Diseases, Tokyo, Japan, and the National Institute of Biomedical Innovation, Osaka, Japan.

Genomic PCR

Hepatic DNA was extracted from homozygous, heterozygous, and wild-type HR mice using an AllPrep DNA/RNA/Protein Extraction Mini Kit (#80004, Qiagen, Hilden, Germany). Primers (Table 1) for PCRs amplifying 15 regions (Fig. 1) in the *Hr* gene were designed based on the *Hr* gene sequence retrieved from the Ensemble database (http://www.ensembl.org). The difference between homozygous (Hr^{x}/Hr^{x}) and wild-type (*Hr/Hr*) genomes was determined using multiple PCRs with HotStarTaq (#203443, Qiagen; regions 1, 8–13) or KOD FX neo (KFX-201, TOYOBO, Osaka, Japan; regions 2–7) DNA polymerases. All PCRs were conducted using a Hybaid Sprint thermal cycler (Thermo Scientific, Waltham, MA, USA) in active-tube control mode. Thermal conditions were as follows: for HotStarTaq, 94°C for 15 min (denaturation and enzyme activation), 40 cycles of 94°C for 10 s, 60°C for 10 s, and 72°C for the appropriate amount of time (see Table 2 for elongation time), and then 72°C for 5 min; for KOD FX neo, 95°C for 2 min, 40 cycles of 98.5°C for 10 s and 68°C for the appropriate amount of time (see Table 2 for elongation time), and then 68°C for 5 min. PCR products were separated in agarose gels: for regions 1 and 8–13, 2% E-Gel EX containing SYBR Safe (G4020-02, Life Technologies, Grand Island, NY, USA); for regions 2–7, 0.5% SeaKem LE agarose gels (#50001, Lonza, Basel, Switzerland) with SB buffer (#SB20-1, Faster Better Media LLC, Hunt Valley, MD, USA) and subsequently stained with GelGreen (#41004, Biotium, Inc., Hayward, CA, USA). Stained gels were photographed with a laser scanner (FX Pro, Bio-Rad, Hercules, CA, USA).

Table 1. List of primers used in this study

Name	Sequence (5'- to 3')
For genome analysis (Fig. 1)	
Int6-F1290	ACCACCCTGGAATCTTCCGTGAAAAA
Int6-R1458	CATGCTTGCTGTGGAGAGTGCGTGCAT
Int6-R539	CACACACGCAGACAAAACTCACTCGT
Int6-R642	TGGCAGTTTATAGCTGTCTGTCACTCTGG
Int6-R850	TGGGCCACCATGGCCAGATTTAACACA
Int6-R979	CACGTGCATGTGTGGACATGTCTGCCTTA
F1843	CGGCTGTGTGTAGCCTGTGGTCGCATA
F1913	AGCACACAGATGACTGCGCCCAGGAG
F193	TTCCTCCAAGGCCCCAAGGACACACTC
F2052	CTGTTTCTGCCAGGTTGATGCCCGTGT
F224	AGAGCGCTGAGCAGAAAGCGGGAGAAC
F2463	GGGCCTGAGCCTTCCATTGTCACCAGT
R1151	TGGCGTGTGAGCCAGGTCTTTTTCAGC
R1873	CGGCTATGCGACCACAGGCTACACACA
R1972	GGGTCAGGATCAGGGAACAGGCAGCAT
R2078	ACACGGGCATCAACCTGGCAGAAACAG
R2433	TGGCCCCAGGGCTTTCTCTTGGATCTT
R3455	AGGCTGGCTCCCTGGTGGTAGAGCTGA
For determining genome sequence in homozygous HR mice (Fig. 2)	
mHR-int6-F514	ACGAGTGAGTTTTGTCTGCGTGT
mHR-int6-R806	CGTAGGTCCTCCTGTTTGCTTGGTCATCA
For genotyping (Fig. 3)	
mHR-mut-S776	GGTCTCGCTGGTCCTTGA
mHR-int6-S607	TCTGGAACCAGAGTGACAGACAGCTA
mHR-int6-R850	TGGGCCACCATGGCCAGATTTAACACA

Table 2. DNA polymerase and elongation time for primer sets in Fig. 1

Primer set in Fig. 1	DNA polymerase*	Elongation time
1	HotStarTaq	5 min
2	KOD FX	3 min
3	KOD FX	6 min
4–7	KOD FX	3 min
8, 9	HotStarTaq	2 min
10–12	HotStarTaq	1 min
13–15	HotStarTaq	30 s

*See Materials and Methods for detailed PCR conditions.

Determination of DNA sequences flanking the insertion site

The genomic region containing the insertion mutation site was amplified by PCR from genomic DNA from homozygous HR mice and a set of two primers, mHR-int6-F514 and mHR-int6-R806 (see Table 1), and KOD-FX neo under the following thermal conditions: 95°C for 2 min, 40 cycles of 98.5°C for 10 s and 68°C for 3 min, and then 68°C for 5 min. PCR products, approximately 13 kbp in length, were gel-purified on a 1% agarose gel, and both the 5' and 3' ends were sequenced using an Applied Biosystems 3730 × l DNA Analyzer (Life Technologies). The obtained sequence was compared to genome databases at the NCBI using a BLAST search.

Genotyping PCR

Primers for genotyping *Hr* alleles were designed according to the sequence information of the alleles (Table 1 for primer sequences; Fig. 3A for primer positions). All three primers were used simultaneously to determine the genotypes of HR and Hos:HR-1 mice. PCRs were conducted using a Hybaid Sprint thermal cycler and HotStarTaq DNA polymerase under the following thermal cycling conditions: 94°C for 15 min, 40 cycles of 94°C for 10 s, 60°C for 10 s, and 72°C for 30 s, and then 72°C for 5 min. PCR products were separated in 2% agarose gels (E-gel EX, G4020-02) and photographed with a laser scanner.

Results

PCR analysis of the Hr allele in HR mice

Analysis of *Hr* alleles in homozygous (H) and wild-type (W) HR mice by means of 15 multiple overlapping PCRs indicated that the Hr^{x} allele contained an insertion mutation in intron 6 (Fig. 1).

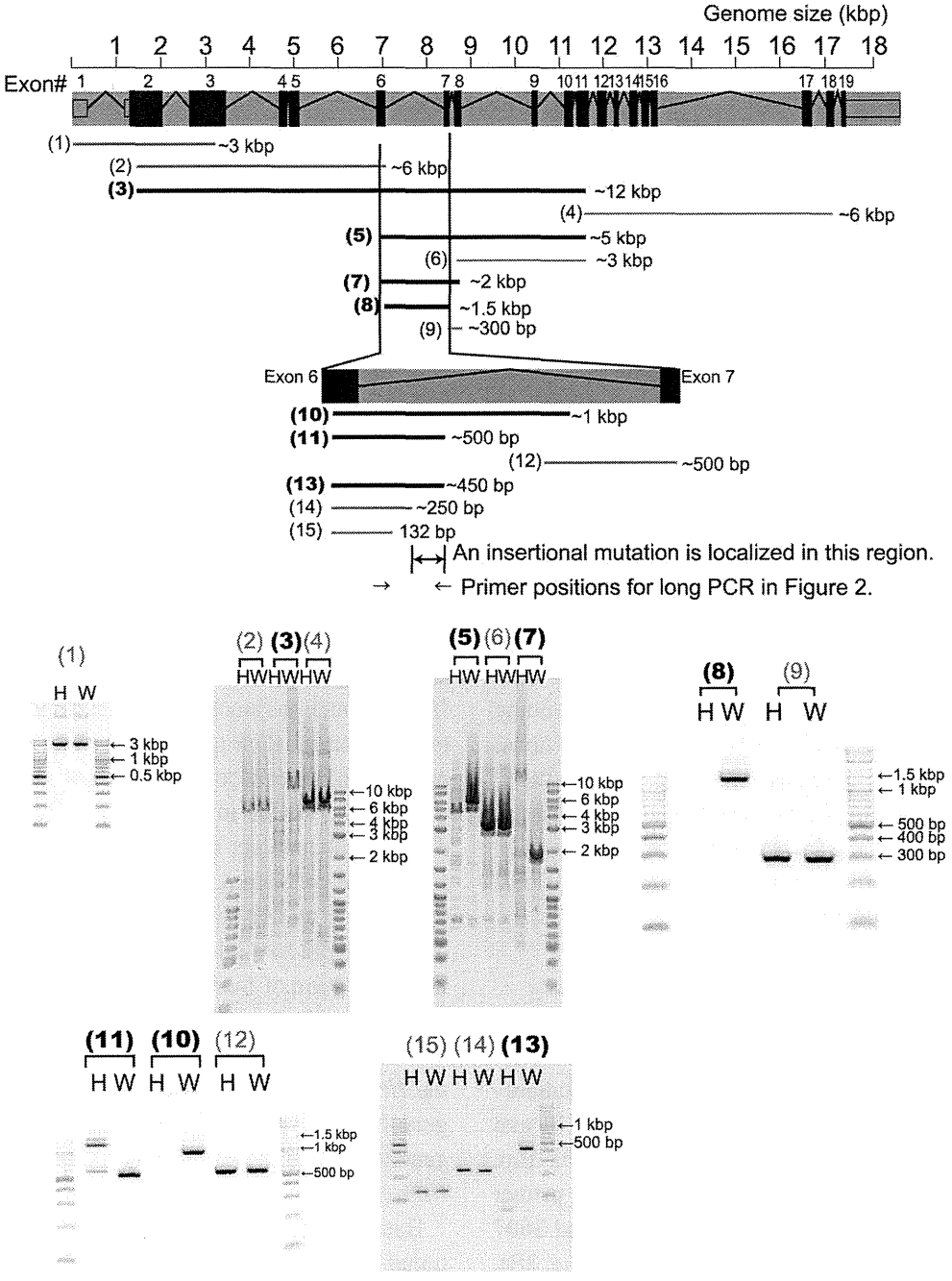

Fig. 1. Analysis of *Hr* alleles in homozygous (H) and wild-type (W) HR mice. The normal (wild-type)*Hr* allele is ~19 kbp in length and consists of 19 exons. A total of 15 overlapping PCRs covering the entire *Hr* coding sequence revealed that an insertion mutation was localized in intron 6 of the Hr^{x} allele. KOD FX neo was used for PCR amplification of regions 2–7, and HotStarTaq was used for PCR of other regions. PCRs shown in gray typeface (1, 2, 4, 6, 9, 12, 14, 15), no difference between homozygous and wild-type HR mice. PCRs shown in black typeface (3, 5, 7, 8, 10, 11, 13), no band or different bands were obtained in homozygous HR mice. Six agarose gel electropherograms show the band patterns of all PCRs. The primer sets used were: (1) F224 and R1151, (2) F193 and R1873, (3) F193 and R2433, (4) F2463 and R3455, (5) F1843 and R2433, (6) F2052 and R2433, (7) F1843 and R2078, (8) F1843 and R1972, (9) F1913 and R2078, (10) F1843 and Int6-R1458, (11) F1843 and Int6-R979, (12) Int6-F1290 and R1972, (13) F1843 and Int6-R850, (14) F1843 and Int6-R642, and (15) F1843 and Int6-R539. The primer sequences and elongation time are shown in Tables 1 and 2, respectively. The primer positions for long PCR shown in Fig. 2 are also indicated in this figure.

Fig. 2. Determination of DNA sequences flanking the insertion mutation in HR mice. PCR with two primers, mHR-int6-F514 and mHR-int6-R806 (positions and sequences are shown in Fig. 1 and Table 1, respectively) produced an ~13-kb-long amplicon containing insertion mutations in homozygous HR mice. Sequencing and BLAST searches indicated that the HR mice share the same insertion mutation as HRS/J mice. The sequences of the 5' and 3' regions flanking the insertion mutation of HRS/J mice were retrieved from GenBank (accession numbers M20235 and M20236, respectively).

Sequencing the mutated region in HR mice

Long PCR for amplifying genomic regions containing the insertional mutation (Fig. 1 for the primer positions) produced an ~13-kb-long amplicon (Fig. 2). Both the 5' and 3' ends of the amplicon were sequenced. Analysis of both sequences using BLAST search revealed that HR mice carried the same insertional mutation as HRS/J mice; i.e., Hr^{x} turned out to be Hr^{hr}.

Genotyping of Hr alleles in HR and Hos:HR-1 mice

Primers for genotyping *Hr* alleles were designed according to their sequence information (see Fig. 3A for primer positions). All three primers were used simultaneously for genotyping PCR. The zygosities of HR and Hos:HR-1 mice were determined using amplicons from both mutant and wild alleles with the following primer sets: S776 and R850 (275 bp, longer bands), and S607 and R850 (244 bp, shorter bands), respectively (Fig. 3B).

Discussion

Our genomic analysis revealed that the HR mice at our institute share the same hairless mutation (Hr^{hr}) as HRS/J and Skh:HR-1 (an ancestor of Hos:HR-1) mice. This indicates that the HR strain is a descendent of the original hairless mice found in London in 1924 [4]. This possibility was also suggested by the fact that the phenotype of HR mice is identical to that of other hairless mice carrying Hr^{hr} alleles. Our genomic analyses confirmed this possibility. Although other mutations of the *Hr* gene, such as rhino (Hr^{rh}) [8] and bald (Hr^{ba}) [6] lead to hairlessness, their phenotypes differ from that of HR mice. Rhino mice become completely hairless by 35 days of age, like HRS/J mice, but older rhino mice have a different phenotype: their skin becomes progressively looser and redundant, forming folds, flaps, and ridges [12]. Rhino alleles contain various types of mutations, different from Hr^{hr} alleles [1, 2]. These mutations result in a truncation of hairless proteins. On the other hand, bald mice are phenotypically intermediate between the hairless and rhino strains [6]. The similarities between the Hr^{hr} and Hr^{ba} alleles are unclear because the bald gene has not yet been sequenced. Thus, HR mice are genetically and phenotypically hairless mice that carry Hr^{hr}.

Based on the genomic sequence around the insertional mutation, we developed a PCR genotyping method. The method was confirmed to be useful for zygosity checks of both HR and Hos:HR-1 strains, and possibly more strains carrying Hr^{hr} alleles. Our three primers flanking the insertional mutation in the Hr^{hr} gene distinguished the zygosities of hairless strains in a single PCR assay. Flanking primer methods [7], often used for the genotyping of transgenes [9], are simple and precise for zygosity determination. Other methods, such as Southern blots and quantitative real-time PCR, are also used for zygosity checks, but are challenging in practice. Both methods use quantitative tests, the results of which are

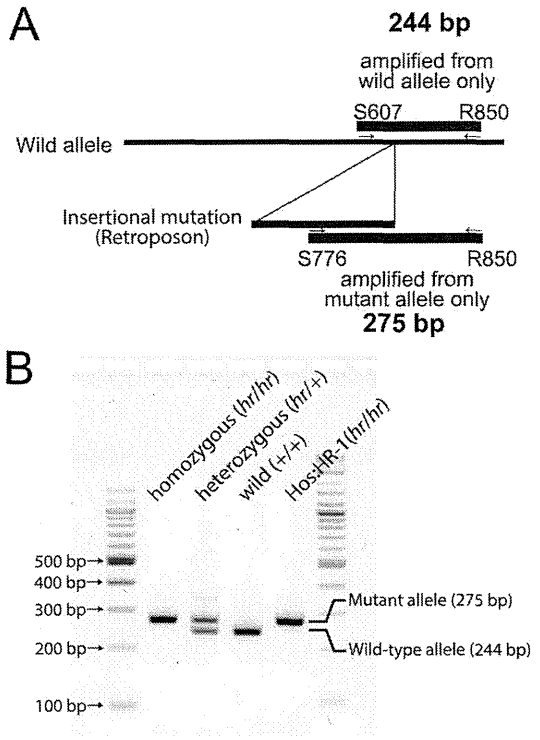

Fig. 3. PCR for genotyping *Hr* alleles in HR and Hos:HR-1 mice. (A) Primer positions (primer sequences are shown in Table 1). PCR using the primers mHR-int6-S607 (S607) and mHR-int6-R850 (R850) produces 244-bp amplicons from wild-type alleles (*Hr*, + in Fig. 3B) only. PCR using the primers mHR-int6-S776 (S776) and mHR-int6-R850 (R850) produces 275-bp amplicons from mutant alleles (Hr^{hr}, *hr* in Fig. 3B) only. (B) Zygosity determination by PCR. Zygosities of *Hr* alleles were determined by PCR using three primers (S607, S776, and R850) simultaneously. If only 275-bp amplicons were produced, the mice were taken to be homozygous (Hr^{hr}/Hr^{hr}). If only 244-bp amplicons were produced, the mice were wild-type (*Hr*/*Hr*). If both amplicons were produced, the mice were heterozygous (Hr/Hr^{hr}). Electropherograms of PCR products indicate the zygosities of homozygous, heterozygous, and wild-type HR mice as well as homozygous Hos:HR-1 mice.

often difficult to compare precisely. In contrast, the flanking primer method is based on qualitative tests (presence or absence of target amplicons) and is easy to perform with no need for complicated procedures such as hybridization of radioactive probes, precise adjustment of template concentration, and so forth. Our primers are different from those of Schaffer *et al.* [10]. Their primers targeted similar positions but had a lower Tm than our primers. We believe that our primers have an advantage because a higher Tm often leads to better results. In addition, PCR results are highly dependent on thermal controls, such as the block-temperature (i.e., based on the temperature of blocks, not that within PCR tubes) and active-tube controls (i.e., based on the temperature within PCR tubes). PCR using a thermal cycler with block temperature control needs a longer reaction time than PCR with active-tube control. In the present study, we used 10 s for the denature and annealing times in a thermal cycler with active-tube control. If a thermal cycler using block-temperature control is used, a longer period, e.g., 30 s, should be used.

Immature hairless mice can be precisely genotyped using our PCR method before their phenotype (hair coat loss) appears. This would enable the use of such mice for research that requires knowledge of precise zygosities.

In summary, the HR strain at our institute carries the same Hr^{hr} alleles as HRS/J and Skh:HR-1 (Hos:HR-1). Our genotyping method could be used for zygosity checks of various hairless mouse strains that carry Hr^{hr} alleles. This method will facilitate the study of hairless mice, and especially immature mice, the zygosities of which cannot be determined based on appearance alone.

Acknowledgment

This work was supported by a grant from the Ministry of Health, Labour, and Welfare, Japan.

References

1. Ahmad, W., Panteleyev, A.A., Henson-Apollonio, V., Sundberg, J.P., and Christiano, A.M. 1998. Molecular basis of a novel rhino (hr^{rhChr}) phenotype: a nonsense mutation in the mouse hairless gene. *Exp. Dermatol.* 7: 298–301. [Medline] [CrossRef]
2. Ahmad, W., Panteleyev, A.A., Sundberg, J.P., and Christiano, A.M. 1998. Molecular basis for the rhino ($hr^{rh\text{-}\&J}$) phenotype: a nonsense mutation in the mouse *hairless* gene. *Genomics* 53: 383–386. [Medline] [CrossRef]
3. Benavides, F., Oberyszyn, T.M., VanBuskirk, A.M., Reeve, V.E., and Kusewitt, D.F. 2009. The hairless mouse in skin research. *J. Dermatol. Sci.* 53: 10–18. [Medline] [CrossRef]
4. Brooke, H.C. 1926. Hairless mice. *J. Hered.* 17: 173–174.
5. Cachon-Gonzalez, M.B., Fenner, S., Coffin, J.M., Moran, C., Best, S., and Stoye, J.P. 1994. Structure and expression of the hairless gene of mice. *Proc. Natl. Acad. Sci. USA* 91: 7717–7721. [Medline] [CrossRef]
6. Garber, E. 1951. hr^{br} – bald. *Mouse News Lett.* 5: 10.
7. Hogan, B., Beddington, R., Constantini, F., and Lacy, E. 1994. Manipulating the Mouse Embryo: A Laboratory Manual, Cold Spring Harbor Laboratory Press, Woodbury.
8. Howard, A. 1940. "Rhino," an allele of hairless in the house

mouse. *J. Hered.* 31: 467–470.
9. Noguchi, A., Takekawa, N., Einarsdottir, T., Koura, M., Noguchi, Y., Takano, K., Yamamoto, Y., Matsuda, J., and Suzuki, O. 2004. Chromosomal mapping and zygosity check of transgenes based on flanking genome sequences determined by genomic walking. *Exp. Anim.* 53: 103–111. [Medline] [CrossRef]
10. Schaffer, B.S., Grayson, M.H., Wortham, J.M., Kubicek, C.B., McCleish, A.T., Prajapati, S.I., Nelon, L.D., Brady, M.M., Jung, I., Hosoyama, T., Sarro, L.M., Hanes, M.A., Rubin, B.P., Michalek, J.E., Clifford, C.B., Infante, A.J., and Keller, C. 2010. Immune competency of a hairless mouse strain for improved preclinical studies in genetically engineered mice. *Mol. Cancer Ther.* 9: 2354–2364. [Medline] [CrossRef]
11. Stoye, J.P., Fenner, S., Greenoak, G.E., Moran, C., and Coffin, J.M. 1988. Role of endogenous retroviruses as mutagens: the hairless mutation of mice. *Cell* 54: 383–391. [Medline] [CrossRef]
12. Sundberg, J.P. 1994. Inbred laboratory mice as animal models and biomedical tools: general concepts. pp. 9–19. *In*: Handbook of Mouse Mutations with Skin and Hair Abnormalities: Animal Models and Biomedical Tools. (Sundberg, J.P. ed.) CRC Press, Boca Raton.
13. Sundberg, J.P. and King, L.E. Jr. 2001. Morphology of hair in normal and mutant laboratory mice. *Eur. J. Dermatol.* 11: 357–361. [Medline]